

See discussions, stats, and author profiles for this publication at: <https://www.researchgate.net/publication/289084534>

Static balance based rescue robot navigation algorithm in random step environment

Article · January 2013

CITATIONS

0

READS

16

2 authors, including:



Evgeni Magid

Kazan (Volga Region) Federal University

114 PUBLICATIONS 787 CITATIONS

SEE PROFILE

Some of the authors of this publication are also working on these related projects:



Control system for robotic laparoscopic instrument [View project](#)



Research and Development of Software Solutions for Static and Dynamic Based Control of Anthropomorphic Bipedal Robots Locomotion [View project](#)

Static Balance based Rescue Robot Navigation Algorithm in Random Step Environment

Evgeni Magid and Takashi Tsubouchi

Intelligent Robot Laboratory, Department of Intelligent Interaction Technologies, University of Tsukuba, Tsukuba, Japan

Keywords: Path Planning, USAR, Rescue Robot, Random Step Environment.

Abstract: To increase safety and extend human rescuers capabilities during a rescue mission a robot is deployed at a rescue site for exploration purposes. To improve a teleoperated rescue robot performance, we develop an automatic pilot system which recommends an operator a safe path to a chosen target. We manage the proposed path from static balance standpoint, based on our previous works. This paper concentrates on path search algorithm in a simulated 3D debris environment, called Random Step Environment.

1 INTRODUCTION

Rescue robotics goal is to perform tasks in hazardous or unreachable by humans environments. One particular domain is urban search and rescue (USAR) which deals with trappy debris of collapsed constructions, and often buried in unreachable locations victims. The catastrophe at Fukushima I nuclear power plant emphasized the indispensability of rescue robots in high radioactive contamination environments, preventing human personal to perform any task.

During USAR mission a rescue robot explores a post-disaster debris site, being operated by a human teleoperator from a safe place outside the site. To decrease pressure on a teleoperator in a path planning stage, we develop a pilot system which helps the operator to select a fairly safe path to a chosen target.

Rough terrain navigation system must be able to decide if a patch ahead is traversable, or it is an obstacle to be circumnavigated (Ye and Borenstein, 2004). To estimate a terrain patch, Gennery (Gennery, 1999) fits planes to the terrain and computes a driving cost, an accumulating traveled distance, and a probability that the slope or roughness may be too large to be traversed. Seraji and Howard (Seraji and Howard, 2002) navigate using terrain local patch roughness, slope, and discontinuity to represent the traversability. Kelly (Kelly, 1995) constructs a 2.5D elevation map and analyzes tip-over, collision, roll and pitch values along a candidate path. Morphin system (Singh et al., 2000) maps sensory data into a 25x25 cm cell size grid, and the goodness of each cell is defined with roll, pitch, and roughness measures. Cell groups form a

goodness map used for evaluation of a predetermined candidate arcs set to choose the best trajectory.

The above approaches are suitable for environments with smooth slopes mainly and are inappropriate for typical post-disaster debris scenes with a significant number of surface discontinuities, which may result into drastic differences between two consequent robot postures. In this paper we present a path search algorithm created specially for the navigation in Random Step Environment (RSE) – a standardized by NIST 3D simulated debris environment (Jacoff et al., 2000). The uniqueness of our approach is the management of a path search for a crawler vehicle in RSE from a balance point of view which is usually associated with legged locomotion (Zucker et al., 2010; Belter and Skrzypczynski, 2012). To make path search feasible we discretize robot movement and state space before the search. The pilot system predicts and categorizes a robot posture at each step of the path with regard to robot static balance. Next, we apply a modification of Depth-First Search algorithm for a path search and dynamically construct a search tree using the rules which we had described in (Magid et al., 2011).

The rest of the paper is organized as follows. In Section 2 we describe our system and simulated environment model. Section 3 presents posture categorization with regard to static stability. Section 4 deals with transitions between consecutive states. The heart of the paper is Section 5 which describes the path search algorithm. Section 7 presents the discussion of our future work. Finally, we conclude in Section 8.

2 SYSTEM SETUP

We assume a tractor-like crawler robot model with a centroidal center of mass location (CoM) which corresponds to the basic configuration of Kenaf robot without the sub crawlers (Fig.1). Kenaf is developed by NEDO project (Yoshida et al., 2007), and it is admitted to have "the best mobility in the world using NIST/ASTM rescue robot evaluation field" (Tadokoro, 2008).

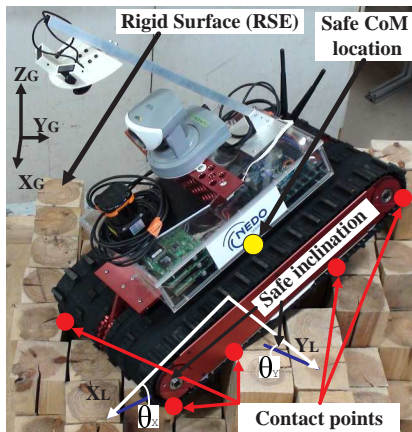


Figure 1: The safety requirements (Conditions A) on the robot posture while operating in RSE.

For our research we use a Random Step Environment (RSE) - a standard NIST/ASTM environment for robot mobility evaluation within RoboCup Rescue framework (Jacoff et al., 2011). We assemble RSE from 85mm \times 85mm size wooden blocks of 0, 90, 180, 270, or 360 mm height (Fig.1). We assume that a small size local map of RSE is always available to the robot¹. To reduce the number of search directions, we discretize the robot movement and the state space before the search. In (Magid and Tsubouchi, 2010) we showed that discretizing each 85x85 mm RSE block (XY-coordinates) into 5x5 internal robot map cells with 17x17 mm size is the best practical choice for our framework. With this discretization, a translation step is a one cell length step in the robot local frame's axis X_L direction (Fig.1); a rotation step is a 5 degrees change in the robot orientation θ , rotating clockwise (right) or counter clockwise (left). This way we significantly reduce the possibility of ending in different from the expected poses when applying small steps in the control.

¹Our application simulates a locally visible part of the environment for a given robot posture, sensor range and global map. For the explanation purposes only we show full local maps.

3 POSTURE CATEGORIZATION

To guarantee reliable motion, a robot is required to be stable at each posture. Using a linear projection approach for static stability estimation (Bretl and Lall, 2008), we define appropriate posture K of the robot (Fig.1) with **Conditions A**:

1. Both crawlers contact terrain with no contacts in the gap between them, thus avoiding getting stuck
 2. Exist at least three distinct contact points
 3. No slipping/overturning due to surface inclination
 4. No overturning due to robot's CoM displacement
- If at least one of Conditions A is not satisfied at posture K , posture K is not appropriate.

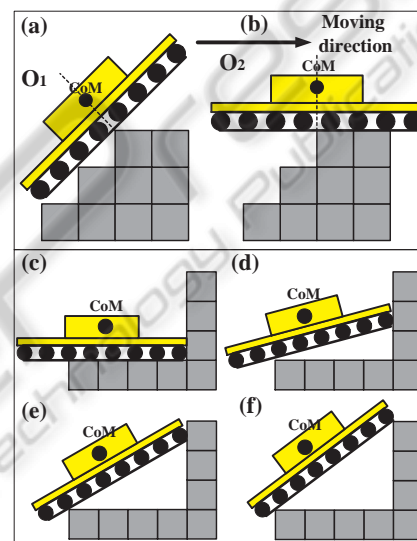


Figure 2: Controlled balance losing (CBL) at Orange state: posture changes from O_1 (a) to O_2 (b). M-chain at climbing up from (c) to (f).

From static stability standpoint we distinguish six posture types, presented in Table 1. **Red** is a prohibited posture. **Cyan** denotes a jump down. Normalized Energy Stability Margin (NESM) (Hirose et al., 1998) is applied to distinguish between two statically stable states: high (**Green**) or fair quality balance (**Yellow**). An unstable **Orange** posture affords to traverse obstacles with losing balance twice on a top: at a barrier edge the robot changes its posture O_1 (Fig.2a) discontinuously and reobtains a balance in a different body orientation O_2 (Fig.2b) as a result of inertia. This controlled balance losing (CBL) state is indispensable for the path planning (Magid et al., 2010). **Magenta** state denotes an ascend/descend on a vertical RSE slope; we define **M-chain** as a sequence of Magenta postures (Fig.2d,e) between two stable postures (Fig.2c,f). The detailed explanations on the posture categorization could be found in (Magid et al., 2008).

Table 1: The color labels explanation.

Label	Balance quality	Technical details
Red (R)	The robot turns upside down OR Gets stuck	Pitch $> \frac{\pi}{4}$ OR Roll $> \frac{\pi}{6}$ OR At least one of Conditions A is not satisfied
Orange (O)	Controlled balance loosing (CBL)	Two optional postures O_1 and O_2 exist
Magenta (M)	The robot ascends OR descends a vertical slope of RSE	Oscillations in posture estimation algorithm
Cyan (C)	The robot jump down	CoM jump between two stable postures $< 50\text{mm}$
Yellow (Y)	Fair balance	(not (R, O, M or C)) AND (NESM parameter < 1)
Green (G)	Good balance	(not (R, O, M or C)) AND (NESM parameter ≥ 1)

4 TRANSITIONS BETWEEN CONFIGURATIONS

To create a search tree, presented in the next section, we provide a branch cutting function (BCF) $F(Args) = Res$. $Args$ are a current robot configuration and a local environment map. Res is a set of accessible within one step configurations, which are at most three postures: go straight, rotate left or right. BCF uses color categorization and estimation of a particular transition feasibility and quality in order to remove all impossible search directions from the search tree and to define the cost evaluation function.

To decide on legal transitions between two successive states, we use a combination of pitch, roll, and contact point quality parameter.² We built a large set of RSEs and confirmed experimentally the set of rules on translational and rotational steps between two successive postures to estimate particular transition feasibility (Magid et al., 2011). To obtain a proper level of the real world approximation, we implemented the rules in our simulator and executed exhaustive simulations followed by verification experiments. The loop rules-simulation-experiments was repeated multiple times: the rules and the thresholds were updated each time until the correlation between the three stages became satisfactory. All possible pairs of postures, connected with a translational or rotational step, were divided into groups using color categories and pitch/roll/contact parameters. Each group is labeled as possible, undesirable or prohibited category transition with regard to the rules. Within each of these three categories the quality of individual transitions may differ significantly, and it is reflected in path cost function $g(v)$, presented in Section 5.2. A path is formed mainly with possible category transitions. Undesired transitions have a limited appearance within the path, while the usage of prohibited ones is totally prohibited.

²Depends on the angle between robot crawlers and the edges of RSE cells and affects the ability to ascend obstacles, to lose balance at CBL, and to descend safely.

5 PATH PLANNING

To find a good path in RSE we create a search tree by means of our BCF. To speed up the search and provide a fairly good solution, gaining computational performance potentially at the cost of accuracy, heuristic methods are used (Russel and Norvig, 2002). When applied for a tree search, a selective at each decision point heuristic focuses on paths that seem to push the robot closer to the target configuration rather than exhaustively exploring all available options. For a heuristic search algorithm the evaluation function of node v is defined as $f(v) = g(v) + h(v)$, where cost $g(v)$ is the actual cost to reach node v from start S , and heuristics $h(v)$ is the estimated cost of reaching target T . Next we present the search tree construction, cost function definition and our search algorithm.

5.1 Search Tree

A naive branching function for each node opens all three descendant nodes - go straight, turn left/right (Fig.3a) - and the number of nodes explodes exponentially with search depth D , where $D \geq \text{dist}(S, T)$ for a discretized distance between start S and a chosen within a visible patch of the environment target T .

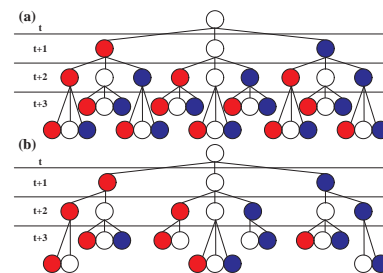


Figure 3: (a) Naive algorithm search tree (NAT) and (b) improved tree (IT) for depth $D=3$. White circle denotes a translational step, red and blue denote rotation left and right respectively.

At first we create an improved tree (IT, Fig.3b) saving one additional node opening at each rotational

Table 2: Good translational transitions cost (in points). P_1 and P_2 are the first and the second postures of the pair.

Label	P_1	P_2	Motion type	$g(v)$
I	G	G	Flat RSE patch	1
II	O	G	CBL, ascend (A)	10
III	G	G	Uniform ascend (UA)	5
	G	G	Uniform descend (UD)	5
IV	O	G	UA after CBL	12
	O	G	UD after CBL	12
V	G	O	CBL, A	10
VI	G	O	CBL at descend	15

step by prohibiting oscillating rotations: immediately after a rotation left a rotation right would be useless, returning the robot to the previous configuration. To reduce further the number of nodes, BCF $F(Args)$ is applied to IT and F -tree (FT) is created – the search tree utilized by our algorithm. At small search depth D naive algorithm tree (NAT), IT and FT have similar number of explored nodes, but as D increases, the difference becomes dramatic (Magid et al., 2011).

5.2 Evaluation Function

Let P_1 and P_2 denote a first (current) and a second (next) posture of a connected by a single step pair respectively. At first, color labels of P_1 and P_2 are calculated, and a transition between P_1 and P_2 is categorized. For a prohibited transition the node is cut off from the search tree with the entire branch that originates at P_1 . Next, for good and undesirable transitions the step cost of transition $P_1 \rightarrow P_2$ is obtained from Tables 2–5. A brief description of the transition type is given in column "Motion type", while the detailed explanations on each transition, including prohibited ones, could be found in (Magid et al., 2011). Finally, column " $g(v)$ " gives the transition cost.

Table 3: Undesirable translational transitions cost (points).

Label	P_1	P_2	Motion type	$g(v)$
VII	G	G	CBL miss, descend(D)	15
VIII	G	G	CBL miss, ascend (A)	10
IX	G	G	M-chain miss, D	20
X	G	G	M-chain miss, A	20
XI	G	G	Non-uniform A	40
XII	G	O	CBL, non-uniform D	100
XIII	M	O	M-chain, D followed by CBL	5000
XIV	G	G	Non-uniform D	100
XV	O	M	CBL followed by M-chain, A	5000
XXIII	M	M	M-chain, A	10
XXIV	M	M	M-chain, D	10

Table 4: Good rotational transitions cost (points).

Label	P_1	P_2	Motion type	$g(v)$
XVI	G	G	Flat patch	5
XVII	G	G	Descending patch (DP)	15
XVIII	G	G	Ascending patch (AP)	20
XIX	G	G	DP with small body orientation change	30
XX	G	G	AP with small body orientation change	40

Table 5: Undesirable rotational transitions cost (points).

Label	P_1	P_2	Motion type	$g(v)$
XXI	M	M	Slide down	1000
XXII	C	G	Jump down	3000

The transition cost was established empirically through the experiment observations taking into account operational complexity, probability of failure due to non-zero friction, sliding, power consumption, etc. The most simple motion is traversing a flat patch of RSE (I). A uniform ascend/descend of a vertical slope (III) and rotation on a flat RSE patch (XVI) require some attention and are more energy consuming. If CBL appears at ascend/descend explicitly (II,V,VI) or implicitly (VII,VIII), a special attention of the operator is needed. CBL at descending (VI,VII) is more dangerous, making such transition to cost a little more; an explicit appearance of CBL in uniform ascend/descend (VI) costs somewhere in between. Transitions XXIII and XXIV denote explicit ascending and descending M-chains respectively. Missed M-chains at descend (IX) or ascend (X) mean faster changes than explicit M-chains and have equal costs: while a fast descend (sliding down) is more dangerous for sensors, ascending a vertical wall consumes more energy and may change robot orientation slightly after completion. Non-uniform ascend (XI) and descend (XIV) intend a CBL appearance; descend is less predictable, as well as an explicit CBL at non-uniform descend (XII). The rotation step is more intuitive - the more body orientation changes, the higher it costs. Also a rotation on a descending slope is easier than on an ascending. Sliding down (XXI) and jumping down (XXII) while rotating are rather unpredictable and thus have high costs in order to avoid their appearances. Finally, two complicated translational transitions XIII and XV receive an extremely high cost, representing a sort of "last chance" for the operator.

For the path planning transitions with cost 1–50 points are mainly used. A number of 100 points cost transitions may postpone the further path exploration for a while. Transitions with cost over 1000 points leave rather small chances for the further exploration of the current path. Yellow category postures are treated in the same way as corresponding green pos-

tures and add 50% penalty to cost $g(v)$. E.g. translation $Y \rightarrow G$ (UA) will cost $5+2.5$ points, while $Y \rightarrow Y$ will cost $1+0.5+0.5$ points.

Heuristic for node v is defined as $h(v) = St_T(v, T) + K \times St_R(v, T)$, where St_T is a number of translation steps from node v to target T on a straight line, and St_R is a number of necessary rotation steps to align orientation θ at node v configuration with the target orientation. We varied heuristic functions from the ones forcing the robot to search within a limited sector first (i.e. concentrated on keeping direction to T) with large parameter K to $K=0$ for distance importance only. Finally, to ensure that the heuristic function will be always admissible, we set $K=0$. Since for the rescue task it is enough to arrive to the target destination more or less precisely, the orientation is less important if we converge in the terms of distance.

5.3 Path Search Algorithm

The most famous heuristic search algorithm is probably A^* - a best-first search type algorithm (Hart et al., 1968) which always finds an existing optimal path but has exponential time and space requirements. Modifications of A^* , like Iterative deepening A^* (IDA^*), reduce space requirements to linear (Korf, 1985), but unfortunately, all variants of A^* at each step select and expand a most high potential node in terms of function $f(v)$. Thus, successively expanded nodes v_i and v_{i+1} are not necessarily adjacent. The class of graph search algorithms, which avoid such undesirable jumps, is Depth First Search algorithm (DFS). DFS (Russel and Norvig, 2002) is the uninformed search that progresses by expanding the search tree in depth in the first child node direction until a goal node or a node without children is reached. In the later case the search backtracks and returns to the most recent node it did not finish.

We have chosen DFS algorithm for our application since we strongly believe that it would converge fast to the target if the path exists. However, to signal that the path does not exist after exploring the entire tree takes the same time as any other tree search algorithm. Often the search graph is too large for the entire exploration, and in such cases DFS would suffer from non-termination. Therefore, when the appropriate depth limit is not known in advance, the search may be performed by iterative deepening, applying DFS repeatedly with a sequence of increasing depth limits. In addition, DFS is much easier to integrate with heuristic methods of choosing a prospective search direction. We make two improvements to iterative deepening DFS and call it MDFS-R - a Modified DFS for Rescue:

- Switch a search direction when the current path becomes unsatisfactory
- Use heuristics to ensure the preference of a more promising search direction

5.4 MDFS-R Algorithm

Similarly to DFS, our algorithm at each node of FT search tree expands 3 (or 2) descendant nodes and chooses the most prospective descendant direction with regard to evaluation function $f(v)$ to continue the exploration of the search tree.

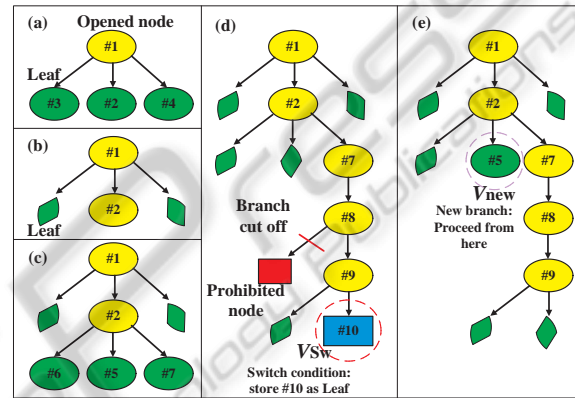


Figure 4: MDFS-R algorithm search tree with the encountered nodes distribution to Leaves (green), Open (yellow) and Prohibit (red) lists.

Figure 4 demonstrates MDFS-R algorithm. We start at node #1, open and evaluate its 3 children - Leafs (Fig.4a, green ovals). Nodes can have 1 (Fig.4d, node #7), 2 (node #9) or 3 (node #1) children. Next, the node is stored in Open list (yellow ovals). If a child node is categorized as red during the evaluation, it is cut off from the search tree and stored in Prohibit list (Fig.4d, red rectangular). Among those children a most promising in terms of minimal cost and heuristics $g(v)+h(v)$ node is chosen to continue the search while others are stored as Leafs (Fig.4b). This procedure is repeated (Fig.4c) until the target is reached³ or a switch condition (explained in the next paragraph) is triggered (Fig.4d, node #10). The node, which triggered the switch, is stored as a Leaf (Fig.4e). The search continues in a different direction starting at a most promising leaf v_{new} (Fig.4e, node #5), which minimizes the cost function with inflated heuristic $g(v)+10 \times h(v)$. Arrival to a dead end activates a backtracking mechanism identical to the one of DFS.

MDFS-R switches the search direction at node v_{sw} in the three following cases:

³Or returning to the start if the path does not exist

1. Path cost $g(v)$ becomes too high: the path became too long or/and contains a large number of undesired transitions reflected in its cost. Exceeding Sw_C threshold signals that the robot seems to be on a wrong path and has to change the search direction. Initially we set $Sw_C = 1.5 \times St_T(S, T)$, where $St_T(S, T)$ is a number of translational steps from Start to Target. After this switch is triggered, Sw_C is reset to $1.5 \times g(v_{new})$, where $g(v_{new})$ is the path cost from Start to the selected leaf v_{new} . This switch condition is updated throughout the search after every switch.
2. Significant **number** of undesired transitions appears within the path; this threshold is set to $Sw_U = 20$. It signals that the path became rather complicated and a human teleoperator may have difficulties to repeat it.
3. The current search direction starts to move the robot away from the desired target. We set this threshold $Sw_H = 1.5 \times St_T(S, T)$.

When one of the three target variables exceeds its threshold, the path becomes undesirable and its further exploration is postponed. If all available choices violate a switch constraint, after choosing the most promising node the corresponding threshold is increased. While Sw_C and Sw_U may only increase during the path search, Sw_H is reset to $1.5 \times St_T(v_{new}, T)$ after every switch. MDFSR can switch back to any of the postponed paths later.

Each node v of FT search tree contains key information $[x, y, \theta]$, posture information $[z, \theta_x, \theta_y]$, NESM, support polygon square, color], pointers to ancestor node $PF(v)$ and three children nodes - go straight $PS(v)$, rotate left $PL(v)$ and right $PR(v)$, heuristic estimation $h(v)$ from v to target T , path cost $g(v)$ from start S to v , and number of undesired transitions $UN(v)$ within that path. We maintain 3 lists of nodes: Opened, Prohibited, and Leaves. Opened list stores explored nodes with expanded children; they may be a part of the successful path. Nodes that were categorized as "red" are cut off from the tree without further exploration of the forthcoming branch, stored in Prohibited list, and do not appear in FT. If after exploration a leaf was evaluated as leading to a dead end, it shifts from Opened list into Prohibited list. Leaves which do not belong to any path yet, are filled up with internal information and stored in Leaves list with $PS(v)=PL(v)=PR(v)=NULL$. When a new node is just opened its key is verified against Opened, Prohibited, and Leaves lists to prevent multiple explorations.

If during the search one of the three switching conditions is triggered while comparing $h(v)$ to Sw_H , $g(v)$ to Sw_C , and $UN(v)$ to Sw_U , the node of the switch (fig.4d, node #10) is stored in Leaves list and

the current candidate path exploration is postponed. A better search direction with regard to the three switch parameters is chosen (node #5) minimizing $g(v)+10 \times h(v)$, and a different candidate path exploration begins. If no better node with regard to current Sw threshold values exists in Leaves list, the violated threshold(s) is(are) increased as was explained earlier. When the target is reached, the path is backtracked through $PF(v)$ pointers.

6 SIMULATION

The search algorithm was implemented in MATLAB environment. Figures 5 and 6 present two simple examples which demonstrate MDFSR behavior in typical situations. For the demonstration purposes only we assumed a full knowledge of a large local RSE patch while usually for a real USAR task the patch size is significantly smaller. When the obstacle between S and T is passable but short, or on the contrary, the obstacle is impassable – the algorithm decides to get round instead of climbing up (Fig.5). When the obstacle is passable but very long, or it cannot be circumvented for some reason, the algorithm chooses to traverse the obstacle (Fig.6). Each cell of the XYZ-grid corresponds to RSE cell. The blue rectangular shows the robot at each distinct posture of the discretized path and the color dots (placed at the robot's CoM) denote static balance category labels.

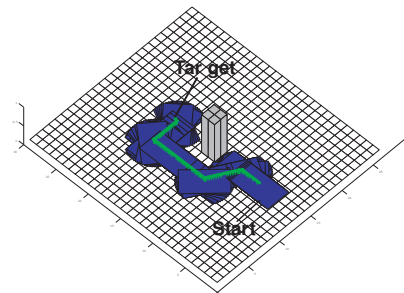


Figure 5: The robot denoted with blue rectangular circumvents small size or impassable obstacles.

Avoiding a pole like obstacle (Fig.5) is a rather trivial task for a human operator, especially under perfect information simulations. The second task of crossing a ridge line (Fig.6) doesn't appear very challenging as well since there are a large number of equally good paths to choose from. So these typical tasks an experienced teleoperator would perform well without any supporting pilot system.

Figures 7 and 8 present the map created with a random generator and randomly chosen start and tar-

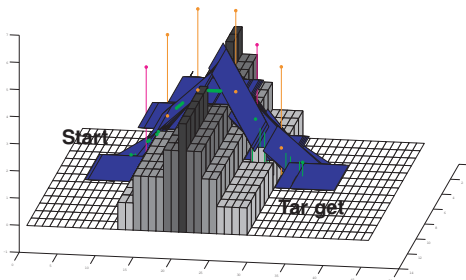


Figure 6: The robot climbs the passable obstacle. The obstacle cells are marked with the grey color: the darkest are 4 units high, the lightest are 1 unit. The 0 high white cells correspond to free space.

get points. While after a number of trials a human operator would probably end up with the robot tip-over, our pilot system succeeded to find a complicated path in RSE with type I translation and type XVI rotation steps only. Except few fair balance postures (yellow dots) within the path, good balance (green dots) is guaranteed along the path and no changes in pitch and roll are involved, preserving horizontal orientation of the robot.

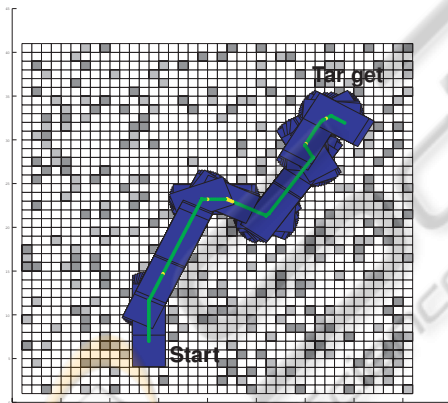


Figure 7: A complicated scenario in the random map (view from above). The RSE cells have 2 (dark grey), 1 (light grey), and zero (white) unit height.

7 FUTURE WORK

Due to the nature of debris scenarios, using in some sense deterministic transitions based on discretized controls is a strong assumption. The transition between states may become unreliable due to the kind of terrain, drift, slippery, etc. As a part of our future work we are going to model the possibility of ending in different from the expected poses when applying

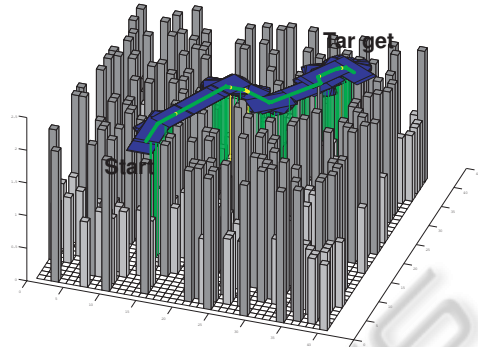


Figure 8: The robot succeeds to find a path preserving horizontal orientation along the path.

a control. Next, we plan to compare MDFS-R algorithm effectiveness with a number of existing planners. While by construction MDFS-R is performing better than classical BFS, DFS, and A^* in terms of average number of opened nodes, we are interested to compare MDFS-R and advanced modifications of A^* , e.g. IDA^* (Korf, 1985) or ARA^* (Likhachev et al., 2004), using different inflated heuristics.

MDFS-R algorithm is targeted to search a locally suboptimal path to a target, which satisfies USAR task, without reconstructing a global map of the environment, and the possibility that the constructed search tree would be used once again for the next stages of USAR mission is relatively small. Yet, if for some reason the robot will have to return and replan, some parts of previously constructed search tree could be reused if we continuously construct and maintain the global map of the rescue scene.

The presented in this work results strongly depend on the considered hardware of KENAF robot, but the proposed approach may be reused at some degree with a different hardware setup. As a part of our long term goal we are interested to apply the proposed research framework for the assistant path selection system development with several other robotic platforms. We plan to build system prototypes followed by real time application development, including global map construction and sensory input treatment.

8 CONCLUSIONS

In this paper we presented static balance based path search algorithm in Random Step Environment for a crawler robot. To make the search feasible, we discretized robot movement and state space before the search. Our modification of Depth-First Search al-

gorithm, targeting specially for path planning tasks of USAR scenarios, dynamically constructs a search tree and provides a fairly safe path to a chosen by the operator target. The simulations showed that while in simple scenarios an experienced operator can manage the path planning process easily, our assistant pilot system is critical in complicated scenarios.

Even though the presented solution deals only with a static stability of the vehicle and suffers from a number of drawbacks and limitations like strong assumptions on rigid and stable RSE, absence of slipperiness and external disturbances, centroidal location of robot's CoM, etc., we believe that our unique approach to the crawler robot path planning from static stability standpoint makes a significant contribution to the rescue robotics domain. While the presented results strongly depend on the considered hardware, the proposed approach may be reused at some degree with a different hardware setup. This way we created a complete framework which could guide assistant system development for any typical crawler vehicle operating in USAR scenario.

ACKNOWLEDGEMENTS

This work was partially supported by NEDO Project for Strategic Development of Advanced Robotics Elemental Technologies, High-Speed Search Robot System in Confined Space. Special thanks are extended to Leave a Nest Co. Ltd., Japan, for the generous financial support of this work.

REFERENCES

- Belter, D. and Skrzypczynski, P. (2012). Posture optimization strategy for a statically stable robot traversing rough terrain. In *IEEE Int. Conf. on Intelligent Robots and Systems*.
- Bretl, T. and Lall, S. (2008). Testing static equilibrium for legged robots. *IEEE Trans. on Robotics*, 24(4).
- Gennery, D. B. (1999). Traversability analysis and path planning for a planetary rover. *Autonomous Robots*, 6(2).
- Hart, P. E., Nilsson, N. J., and Raphael, B. (1968). A formal basis for the heuristic determination of minimum cost paths. *IEEE Trans. on Systems Science and Cybernetics*, 4(2).
- Hirose, S., Tsukagoshi, H., and Yoneda, K. (1998). Normalized energy stability margin: generalized stability criterion for walking vehicles. In *The 1st Int. Conf. on Climbing and Walking Robots*.
- Jacoff, A., Messina, E., and Evans, J. (2000). A standard test course for urban search and rescue robots. In *Performance Metrics for Intelligent Systems Workshop'00*.
- Jacoff, A., Virts, A., and Downs, T. (2011). *RoboCup Rescue Robot League Arenas: Major component descriptions*. Available online: <http://www.isd.mel.nist.gov/projects/USAR/>.
- Kelly, A. J. (1995). *Predictive control approach to the high-speed cross-country autonomous navigation problem*. PhD thesis, Carnegie Mellon University.
- Korf, R. E. (1985). Depth-first iterative-deepening: An optimal admissible tree search. *Artificial Intelligence*, 27.
- Likhachev, M., Gordon, G., and Thrun, S. (2004). *ARA*: Anytime A* with Provable Bounds on Sub-Optimality*. Advances in NIPS, MIT Press, Cambridge, MA.
- Magid, E., Ozawa, K., Tsubouchi, T., Koyanagi, E., and Yoshida, T. (2008). Rescue robot navigation: Static stability estimation in Random Step Environment. In *Int. Conf. on Simulation, Modeling and Programming for Autonomous Robots*.
- Magid, E. and Tsubouchi, T. (2010). Static balance for rescue robot navigation: Translation motion discretization issue within Random Step Environment. In *Int. Conf. on Informatics in Control, Automation and Robotics*.
- Magid, E., Tsubouchi, T., Koyanagi, E., and Yoshida, T. (2010). Static balance for rescue robot navigation: Losing balance on purpose within Random Step Environment. In *IEEE Int. Conf. on Intelligent Robots and Systems*.
- Magid, E., Tsubouchi, T., Koyanagi, E., and Yoshida, T. (2011). Building a search tree for a pilot system of a rescue search robot in a discretized Random Step Environment. *J. of Robotics and Mechatronics*, 23(4).
- Russel, S. J. and Norvig, P. (2002). *Artificial intelligence: A modern approach*. Prentice Hall.
- Seraji, H. and Howard, A. (2002). Behavior-based robot navigation on challenging terrain: a fuzzy logic approach. *IEEE Trans. on Robotics and Automation*, 18(3).
- Singh, S., Simmons, R., Smith, T., Stentz, A., Verma, V., Yahja, A., and Schwehr, K. (2000). Recent progress in local and global traversability for planetary rovers. In *IEEE Int. Conf. on Robotics and Automation*.
- Tadokoro, S. (2008). *Rescue Robotics in Japan*. DHS University Network Summit'2008.
- Ye, C. and Borenstein, J. (2004). A method for mobile robot navigation on rough terrain. In *IEEE Int. Conf. on Robotics and Automation*.
- Yoshida, T., Koyanagi, E., Tadokoro, S., Yoshida, K., Nagatani, K., Ohno, K., Tsubouchi, T., Maeyama, S., Noda, I., Takizawa, O., and Hada, Y. (2007). A high mobility 6-crawler mobile robot Kenaf. In *The 4th International Workshop on Synthetic Simulation and Robotics to Mitigate Earthquake Disaster*.
- Zucker, M., Bagnell, J. A., Atkeson, C. G., and Kuffner, J. (2010). An optimization approach to rough terrain locomotion. In *IEEE Int. Conf. on Robotics and Automation*.